The Assignment of the Different Infrared Continuum Absorbance Changes Observed in the 3000–1800-cm^{-1} Region during the Bacteriorhodopsin Photocycle

Florian Garczarek,* Jianping Wang,† Mostafa A. El-Sayed,† and Klaus Gerwert*
*Lehrstuhl für Biophysik, Ruhr-Universität Bochum, D-44780 Bochum, Germany; and †Laser Dynamics Laboratory, School of Chemistry and Biochemistry, Georgia Institute of Technology, Atlanta, Georgia

ABSTRACT The bleach continuum in the 1900–1800-cm^{-1} region was reported during the photocycle of bacteriorhodopsin (bR) and was assigned to the dissociation of a polarizable proton chain during the proton release step. More recently, a broad band pass filter was used and additional infrared continua have been reported: a bleach at >2700 cm^{-1}, a bleach in the 2500–2150-cm^{-1} region, and an absorptive behavior in the 2100–1800-cm^{-1} region. To fully understand the importance of the hydrogen-bonded chains in the mechanism of the proton transport in bR, a detailed study is carried out here. Comparisons are made between the time-resolved Fourier transform infrared spectroscopy experiments on wild-type bR and its E204Q mutant (which has no early proton release), and between the changes in the continua observed in thermally or photothermally heated water (using visible light-absorbing dye) and those observed during the photocycle. The results strongly suggest that, except for the weak bleach in the 1900–1800-cm^{-1} region and >2500 cm^{-1}, there are other infrared continua observed during the bR photocycle, which are inseparable from the changes in the absorption of the solvent water molecules that are photothermally excited via the nonradiative relaxation of the photoexcited retinal chromophore. A possible structure of the hydrogen-bonded system, giving rise to the observed bleach in the 1900–1800-cm^{-1} region and the role of the polarizable proton in the proton transport is discussed.

INTRODUCTION

The question of whether or not protons are transferred via protonated hydrogen-bonded networks in proteins is of general interest. The membrane protein bacteriorhodopsin (bR), a light-driven proton pump, is a very suitable protein to study proton transfer (for recent reviews, see Haupts et al., 1999; Lanyi, 2000).

Protonated hydrogen-bonded networks are monitored by the so-called continuum absorbance over a broad spectral range covering several hundred wavenumbers in the infrared region. This is shown in experimental and theoretical studies of numerous model systems (Lobaugh and Voth, 1996; Vuilleumier and Borgis, 1999; Zundel, 2000; Kim et al., 2002). To monitor proton transfer via the protonated hydrogen-bonded networks in proteins, broad infrared (IR) absorbance changes >1800 cm^{-1} are investigated during the photocycle of bR. This spectral region is used because proteins do not absorb here (Olejnik et al., 1992; Le Coutre et al., 1995; Riesle et al., 1996; Rammelsberg et al., 1998; Wang and El-Sayed, 2000).

Using a band pass filter with a cutoff frequency at 1950 cm^{-1}, Rammelsberg et al. showed that the kinetics of the integrated negative absorbance (bleach) between 1900–1800 cm^{-1} was correlated with the proton transfer to the protein surface (Rammelsberg et al., 1998). They concluded that a network of protonated internal water molecules stabilized by Glu-204 and located in a hydrophilic pocket on the extracellular proton release side deprotonates during this process. The idea of the proton release group being a protonated water network was also supported by theoretical studies (Spassov et al., 2001; Rousseau et al., 2004).

A further support was found by Wang and El-Sayed from the observed correlation between the temporal bleach behavior of the changes in the 1850–1800-cm^{-1} region and the protonation of the COO^- group of Asp-85 during the bR photocycle as well as by the fact that the observed changes in this region do not occur in D_2O (Wang and El-Sayed, 2000). In a latter publication, Wang and El-Sayed expanded their studies to a broader frequency range by using a band pass filter with a cutoff at 3000 cm^{-1} (Wang and El-Sayed, 2001). In this study additional continua were reported: a transient bleach >2700 cm^{-1}, a transient bleach in the 2500–2150-cm^{-1} region, and an absorption (not bleach) is observed in the 2100–1800-cm^{-1} region. These continua have time constants of ~300 μs, which could not be correlated to the characteristic time constants of the different processes monitored due to the changes in the retinal or protein absorption in the reaction center. The origin of these continua remains unassigned. The low energy continuum in the 2100–1800-cm^{-1} region is found to have in addition a 60-μs component correlated with the L→M transition as first proposed by Rammelsberg et al. (1998). However, the fact that the continuum was absorptive rather

Submitted May 25, 2004, and accepted for publication July 19, 2004.

Address reprint requests to Klaus Gerwert, Lehrstuhl für Biophysik, Ruhr-Universität Bochum, D-44780 Bochum, Germany. Tel.: 49-234-32 24461; Fax: 49-234-32 14238; E-mail: gerwert@bph.ruhr-uni-bochum.de.

Jianping Wang's present address is Dept. of Chemistry, University of Pennsylvania, Philadelphia, PA 19104-6323.

0006-3495/04/10/2676/07 $2.00

doi: 10.1529/biophysj.104.046433

than bleach (as observed by Rammelsberg et al.) would suggest that the polarizable proton chain is formed during the cycle (in <90 ns) before the K intermediate and then decays during the L→M transition. If it is a bleach signal, then the chain is present in the bR ground state (BR) and deprotonates during the L→M transformation.

To elucidate the exact mechanism of the proton transport during the bR function, it is important to assign the origin of the continua observed during the bR photocycle. Furthermore, it has to be determined whether the polarizable proton chain is already present in the parent molecule of bR and breaks during the proton pump, or is formed and breaks during the photocycle. Hence it is essential to determine the exact sign of the change in the 1900–1800-cm^{-1} region.

This work is aimed at getting answers to these questions. The time-resolved experiments were carried out on the bR-E204Q mutant, which has no early proton release (Brown et al., 1995). Furthermore, the frequencies of the different continua are compared with the Fourier transform infrared spectroscopy (FTIR) spectrum of water and of the resulting difference spectra observed when heating liquid water by as little as 0.2°C. In addition, a time-resolved measurement of a water-dye mixture was made to examine the influence of photothermal heating of water. The results were compared with those obtained during the wild-type bacteriorhodopsin (WT-bR) photocycle. These results suggest that all the continua observed, except for the weak bleach in the 1900–1800-cm^{-1} region and >2500 cm^{-1}, are dominated by transient signals coming from photothermally heated water during the photocycle. The weak band in the 1900–1800-cm^{-1} region is found to be a bleach band, but due to its overlap with the hot water absorptive band on its high energy side makes its apparent sign sensitive to the amount of water in the film, the film thickness, the laser power, and the type of filter used. The structure of the water complex, whose spectrum changes during the L→M transformation (in the 1900–1800-cm^{-1} region), is proposed and its role in the proton transport is discussed.

MATERIALS AND METHODS

Sample preparation

bR sample: 0.1 mg of pure membrane sheets were suspended in 1M KCl and 100 mM Tris-HCl buffer at pH7, and then centrifuged for 2 hr at 200,000 g to concentrate the sample. The pellet was squeezed between two CaF_2 windows, which were placed in a homemade thermally stabilized sample holder.

Dye sample

A sample consisting of a saturated solution of indigocarmin was prepared and placed in the same sample holder as used in the bR experiment.

Measurements

Time-resolved step-scan FTIR measurements were performed at 20°C on a Bruker IFS66v (Bruker Optik GmbH, Ettlingen, Germany) and a Nicolet (Madison, WI) Magna-IR 860 spectrometer. Spectra were recorded with up to 10-ns time resolution and a spectral resolution of 4–10 cm^{-1}, between 3200 and 800 cm^{-1}. The bR samples were excited by a depolarized Nd:YAG laser at 532 nm (Spectra-Physics (Mountain View, CA) GCR-170), having an energy of 2 (mJ/cm^2)/pulse and a pulse width of 6 ns length. Another Nd:YAG laser (Quantum Ray DCR3, Mountain View, CA) with a laser energy of 3 mJ/pulse and a pulse width of 10 ns was also used. Linear photovoltaic HgCdTe detectors (20–50 MHz, Kolmar Technologies, Newburyport, MA) were used.

RESULTS AND DISCUSSION

Mutant studies in the narrow 1800–1900-cm^{-1} region and at long time

The time-resolved FTIR difference spectra in the region between 1900 and 1740 cm^{-1} between the ground state and taken 1 ms after laser excitation for WT-bR and for E204Q are shown in Fig. 1 *A*. The 1-ms spectrum represents a mixture of the M and N intermediate (M/N). At 1762 cm^{-1} the protonation of Asp-85 in M/N is observed. In WT a proton is released in the L→M transition to the protein surface (Heberle and Dencher, 1992), which is accompanied by a negative continuum absorbance change (bleach) between 1900 and 1800 cm^{-1}. In E204Q, the proton release is inhibited during the L→M transition and the continuum absorbance change is no longer observed. These results support the previous conclusions that absorbance changes in this region result from the proton pump process during the L to M transition.

Fig. 1 *B* shows a comparison of the time course for WT and E204Q, integrated between 1900 and 1800 cm^{-1}. The time course of WT can be resolved into at least three exponential functions. They represent the L→M transition, the M→N/O transition, and the N/O→BR relaxation. The negative continuum absorbance change (bleach) is formed in the L→M transition, when the proton is released to the extracellular surface. The released proton may also lead to a change in the hydrogen-bonded network along the surface. However, such changes are not observed here, because such a band should be positive due to its appearance during the M formation. Furthermore the absorbance change of a fluctuating proton on the protein surface might be very small or have different spectral characteristics due to its large mobility. Thus the continuum absorbance change represents the deprotonation of a protonated hydrogen-bonded network of internal water molecules on the proton release site (Rammelsberg et al., 1998), stabilized by Glu-204 and Glu-194 (Spassov et al., 2001). The bleach continuum during the M→N transition is assigned to a proton transfer between Asp-96 and the Schiff base via a hydrogen-bonded network of internal water molecules (Le Coutre et al., 1995). Fig. 1 *B* shows that the bleach continuum is no longer observed for E204Q. In this mutant the proton pump process is inhibited, and one does not expect to observe a change in the polarizable proton absorption during the photocycle. This strongly supports the conclusion that the observed bleach

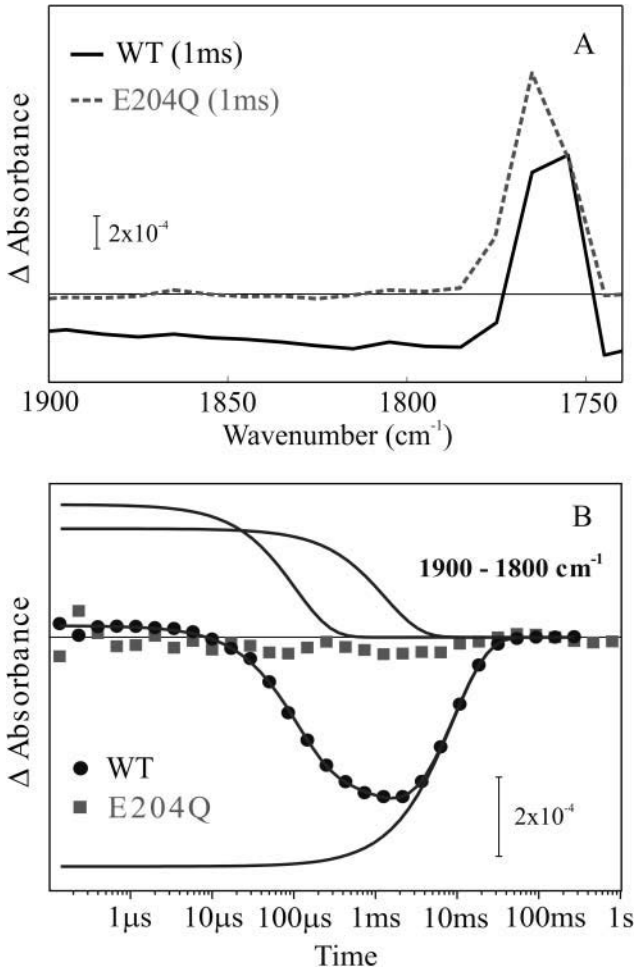

FIGURE 1 Comparison of time resolved FTIR measurements of wild-type bR (*WT*) and the E204Q mutant. (*A*) Difference spectra in the 1900–1740-cm^{-1} region 1 ms after laser excitation. (*B*) Time dependence of the observed spectral change integrated between 1900 and 1800 cm^{-1} for WT (●) and its mutant (■) in the 100 ns–1 s timescale. It appears that although WT shows the formation and decay of a bleach in this region, its mutant, which has no early proton release, does not. This suggests that the absorbance changes in this region are correlated with the proton release in wild-type bR, which occurs within microseconds (Rammelsberg et al., 1998).

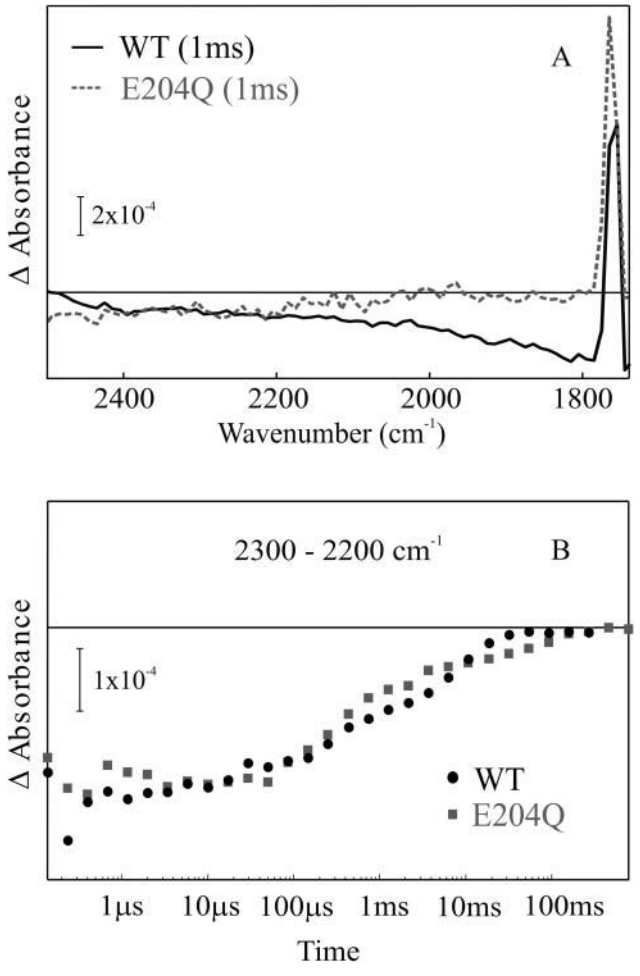

FIGURE 2 (*A*) Comparison of time-resolved FTIR difference spectra between 2500 and 1740 cm^{-1} for WT and E204Q, taken 1 ms after laser excitation. (*B*) Comparison of the time course for WT-bR and E204Q, averaged between 2300 and 2200 cm^{-1}.

during the proton pump process in the 1900–1800-cm^{-1} region is a result of the dissociation of a polarizable proton chain involved in the proton pump process.

Time-resolved mutant studies in the extended region >1900 cm^{-1}

Fig. 2 *A* gives a comparison of time-resolved FTIR difference spectra in the region between 2500–1740 cm^{-1} for WT-bR and E204Q, taken 1 ms after laser excitation. This is the extended region observed by Wang and El Sayed (2001). Comparison of the time course for WT-bR and E204Q, averaged over the 2300–2200-cm^{-1} region, is shown in Fig. 2 *B*.

From Fig. 2 it is found that the absorbance change >2200 cm^{-1} and the kinetics at times longer than 1 ms are the same for WT-bR and E204Q. This is in contrast to what was observed between 1900 and 1800 cm^{-1} (Fig. 1). It suggests that changes in this region are not correlated to the proton release process. The different behavior of the absorbance change between 2500 and 2100 cm^{-1} and between 1900 and 1800 cm^{-1} suggests that they result from different processes.

The origin of the absorbance changes >2100 cm^{-1}

Beside the changes in the 1900–1800-cm^{-1} region, the observed change >1900 cm^{-1} has a decay time of ~300 μs and is observed in a perturbed bR system that has a late proton release. These spectral changes could thus arise from the photothermal heating of either water or the protein.

Fig. 3 *A* shows the FTIR difference spectra in the 2500–1740-cm^{-1} region of a WT sample (*dotted line*) and pure water (*dashed line*) after increasing its temperature by 0.2°C

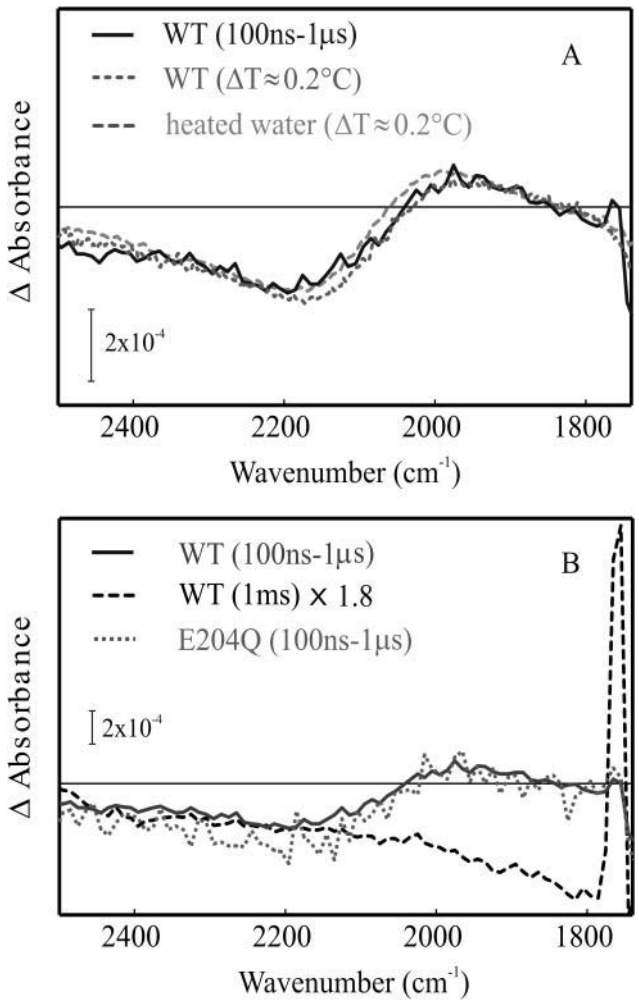

FIGURE 3 (*A*) FTIR difference spectra in the 2500–1740-cm^{-1} region for WT (*dotted line*) and for pure water (*dashed line*) after increasing its temperature by 0.2°C above room temperature and the early transient FTIR spectrum averaged between 100 ns and 1 μs after laser excitation (*solid line*). (*B*) Comparison between an early FTIR difference spectra of WT (*solid line*) and E204Q (*dotted line*) (100 ns–1 μs) and a late spectrum (1 ms) of WT (*dashed line*).

above room temperature. In the same figure the changes in the early transient FTIR spectrum averaged between 100 ns and 1 μs after laser excitation (i.e., before proton release) is shown. In Fig. 3 *B*, a comparison between an early FTIR difference spectrum (100 ns–1 μs) of bR (*solid line*) and E204Q (*dotted line*) (100 ns–1 μs) and a late spectrum (1 ms) of bR (*dashed line*) is presented.

Because the spectral changes in the 2500–1800-cm^{-1} region for WT and the E204Q mutant in the short timescale between 100 ns–1 μs are similar to changes in heated water, these spectral changes might be dominated by absorption changes of water molecules that are photothermally heated as a result of the retinal photoabsorption, followed by non-radiative relaxation during the photocycle. If the spectral changes are recorded at times equal or longer than the proton release (60 μs), the similarity between the changes in heated water and the mutant is observed. This similarity is not observed between heated water and WT in the region between 1900 and 1800 cm^{-1}. This again suggests that the spectral region around 1900–1800 cm^{-1} could be associated with the polarizable protons involved in the proton release process, whereas the spectral changes at 2500–2000 cm^{-1} result from changes in water not involved in the photocycle. Furthermore, it shows that the continuum absorbance change can be separated well from the heat artifact as long as the energy of the exciting laser is low enough. This explains why the absorbance changes in this region as well as in the high energy region (3000–2700 cm^{-1}) have rise times $<$80 ns (the detector time resolution), and all have a decay component of $\sim$300 μs (Wang and El-Sayed, 2001). The conversion of the photoabsorbed energy into heat by retinal is very rapid (subpicosecond), thus $<$80 ns. The 300-μs relaxation component might be assigned to the absorption changes due to the proton chains in water, in the water-protein complex or merely in the protein, resulting from the heat pulse that is photothermally produced. However, it cannot be unambiguously ruled out yet the possibility that these $\sim$300 μs transient components may be involved in proton translocation one way or the other, simply because they appear to be on the timescale between μs to ms, on which the two photo-intermediates M and N are identified. A detailed picture in protein interior on this timescale is still missing.

The spectrum of heated water

To reveal the exact spectral behavior of the artificial IR signal, which overlaps the time-resolved bR measurements, we performed a time-resolved step-scan measurement of a water-dye mixture. The dye (indigocarmin) only functions as a light absorber for heating the water. Fig. 4 *A* shows the time courses of four different spectral ranges of this measurement. The ns-change in the signal is due to the detector rise. The absorbance change observed within $\sim$20 μs is due to the relaxation of hot water to its initial state. This is faster in the water sample (water + dye) than in the bR sample (bR + water) due to the high heat conductivity of ''pure'' water and the lower sample thickness.

The integrated spectrum between 100 ns and 3 μs is shown in Fig. 4 *B* (*dotted line*), and it is compared with a time-resolved BR-L spectrum taken 3 μs–10 μs after light excitation (*solid line*). The time course of the integrated 1900–1800-cm^{-1} region (*II*) demonstrates that no artificial signal overlaps with the spectral region used to detect the time behavior of the continuum absorbance change.

The assignments of the different continua

Fig. 5 *A* shows an absorbance spectrum of native bR in H_2O at pH $\sim$7. The spectrum reveals a broad band with a maximum at $\sim$2140 cm^{-1} (Fig. 5 *A*). This band is due to

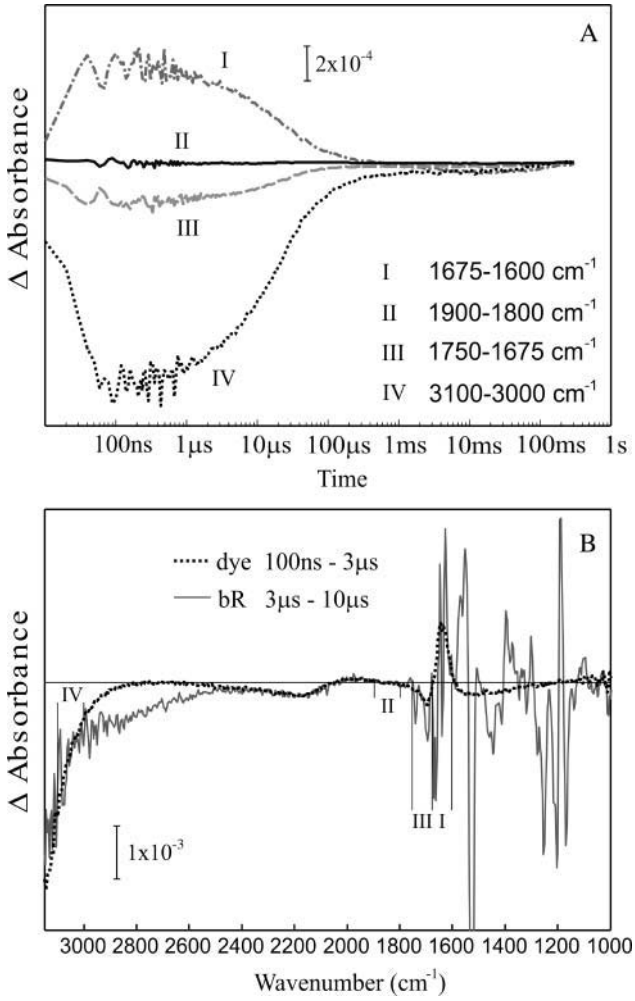

FIGURE 4 Time-resolved step-scan measurement of photothermally heated water-dye mixture. (*A*) Time courses of four different spectral ranges. The spectral region used to detect the continuum absorbance change (1900–1800 cm^{-1}) is not disturbed by the heat artifact. (*B*) Comparison of the transient FTIR spectrum of the water + dye measurement integrated between 100 ns and 3 μs (*dotted line*) and the BR-L spectrum integrated between 3 μs and 10 μs (*solid line*). The water + dye measurement shows the spectral changes resulting from the photothermal heated water, which overlaps the time-resolved bR measurements.

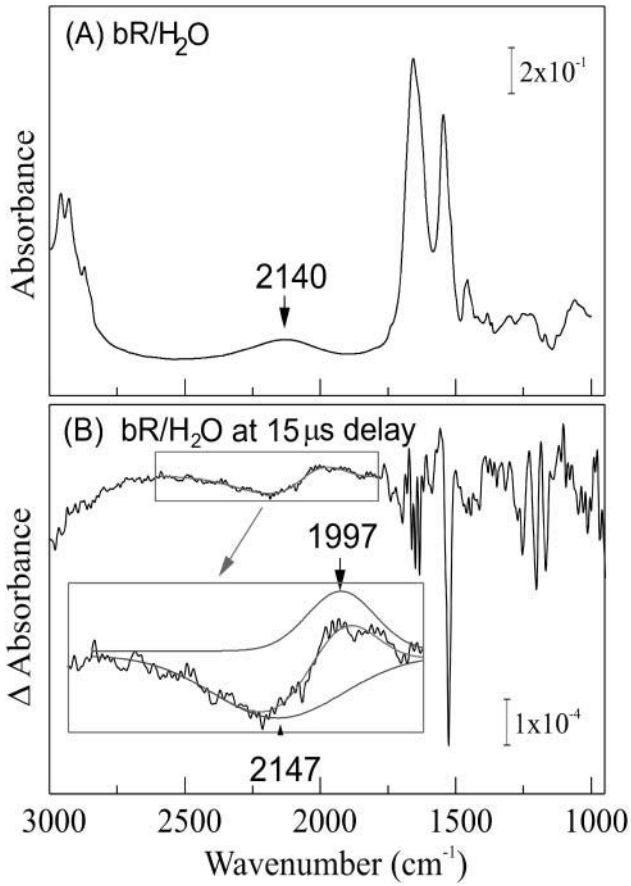

FIGURE 5 (*A*) Steady-state FTIR spectrum at 3000–1000 cm^{-1} of native bR in H_2O. (*B*) Transient FTIR spectrum at 15 μs delay after pulsed laser excitation at 532 nm. In the inset, spectral change in the 2600–1800 cm^{-1} has been deconvoluted into a transient bleach band with a maximum at 2147 cm^{-1} and absorption at 1997 cm^{-1}.

a combination vibrational mode in the H_2O solvent of the bending (~1600 cm^{-1}) and the two librations (L_1 ~ 400 cm^{-1}, L_2 ~ 700 cm^{-1}). Fig. 5 *B* shows the transient spectrum obtained 15 μs after laser excitation of bR at 532 nm with a power level of 1.2 mJ/pulse. In this early time delay the bleach at 1900–1800 cm^{-1} is not formed. The spectral change at 2600–1800 cm^{-1} can be deconvoluted into two bands, one absorptive band with a maximum at ~1997 cm^{-1} (2200–1800 cm^{-1}), and one bleach band in the region 2600–1800 cm^{-1} with a maximum at ~2147 cm^{-1}. A comparison of the two spectra in Fig. 5 suggests that the bleach band at 2147 cm^{-1} and the absorptive band at 1997 cm^{-1} result from the weak combination band of the H_2O solvent. The bleach >2800 cm^{-1} in Figs. 5 *B* and 4 *B* is due to a change of the water O-H stretch absorption seen >2800 cm^{-1} in Fig. 5 *A*. But in addition to the band caused by heated water, there is another broad bleach band between 3000 and 2500 cm^{-1}. This band is identifiable by comparing the time-resolved bR spectrum with a corresponding heated water spectrum as done in Fig. 4 *B*. A broad negative band was also observed in low-temperature FTIR BR-K measurements and proposed to originate from a strong hydrogen-bonded water between the SB and Asp-85 (Kandori et al., 1998; Hayashi and Ohmine, 2000; Tanimoto et al., 2003). The assignment of this broad band at room temperature is not yet clear and needs further experiments. It might correlate with the whole water cluster close to the Schiff base (Kandt et al., 2004; Fig. 6).

The excited retinal chromophore of bR itself appears to act as an efficient light-to-heat converter. The quantum efficiency of the retinal photoisomerization (and photocycle) is ~60% (Tittor and Oesterhelt, 1990). Thus, 40% of the light energy absorbed by the retinal is converted either into heat as a result of nonradiative relaxation or light. The quantum yield of the radiative relaxation has been determined to be

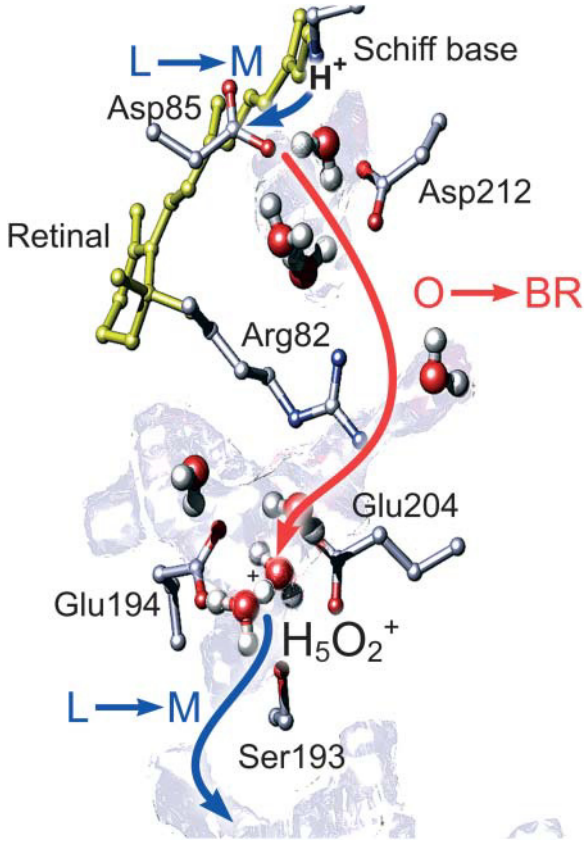

FIGURE 6 Proton release pathway of bR. There are two internal water cavities on the proton release pathway separated by Arg-82 that contain protonated hydrogen-bonded networks. One is close to the Schiff base, Asp-85, Tyr-185, and Asp-212, and the other between Arg-82, Glu-204, and Glu-194. The protonated network of internal water molecules, which is indicated by the continuum absorbance change between 1900–1800 cm^{-1}, is located in the lower cavity and represents the proton release group.

$<10^{-4}$ (Wang and El-Sayed, 2002). This leaves a large amount of heat energy given off during excited state retinal relaxations, resulting in rapid heating of the solvent, whose temperature jump profile can be derived from the kinetics of the bleach band located near 2200 cm^{-1} or >3000 cm^{-1}. Because the nonradiative relaxation of the retinal excited state occurs in the subpicosecond time domain (Song et al., 1993; Logunov et al., 1996) for both WT-bR and E204Q, and the temperature thermalization and diffusion occurs within subnanosecond time domain (Anfinrud et al., 1989), the rise time of the T-jump is determined by the excitation pulse width (~6 ns). The heat released from the retinal is then absorbed by the surrounding protein and water molecules. Actually the rise time of the bleach band at 2147 cm^{-1} has been determined to be <20 ns (data not shown). This heat is finally removed from the monitoring volume in ~300 μs for the bR sample as a result of heat conduction.

This light-to-heat conversion and the temperature reversion could be well reproduced by exchanging bR with a dye. A comparison of these two measurements resolves the broad absorbance changes originally from the bR photocycle and the spectral changes resulting from heated water that are shown significantly in the rest of the bands.

From the above discussion and Fig. 3, *A* and *B*, it is clear that there is a strong overlap between the spectral changes due to the hot water absorptive band in the 2040–1870 cm^{-1} region and the weak bleach band in the 1900–1800 cm^{-1} region. Thus the apparent sign of the 1900–1800 cm^{-1} band will greatly depend on the absorption of the hot water band, which will depend on amount of water (thus the sample preparation), the laser power (the heating rate), the film thickness (the cooling rate), and the filter used to resolve them. We believe some of these effects must have led to the opposite observations reported on the sign of the band in the 1900–1800 cm^{-1} region in the two studies by Wang and El-Sayed.

Structural support of possible proton pump mechanism

Recently, the proposal that a polarizable proton chain (Rammelsberg et al., 1998) is involved in proton release was supported at the structural level. The $H_5O_2^+$ complex is believed to be stabilized between Glu-204 and Glu-194 in the proton release pathway (Fig. 6). This is based on an integrated approach combining high resolution x-ray data, FTIR measurements, pK_a calculations, and molecular dynamics simulations (Rammelsberg et al., 1998; Luecke et al., 1999; Spassov et al., 2001; Kandt et al., 2004). There are two internal water densities within the proton release pathway that might contain protonated hydrogen-bonded water networks at the proton release site. One is close to the Schiff base, Asp-85, Tyr-185, and Asp-212, and the other between Arg-82, Glu-204, and Glu-194. Mutations of residues in the cavity close to the Schiff base do not affect the continuum absorbance between 1900 and 1800 cm^{-1}, but mutations in the lower pocket do (data not shown). Therefore, the protonated network of internal water molecules represented by the absorbance change between 1900 and 1800 cm^{-1} is located in the lower pocket as indicated in Fig. 6.

We thank Nikolaus Bourdos for a critical review of the manuscript, and Christian Kandt for providing the moleculare image.

Mostafa A. El-Sayed and Jianping Wang thank the Chemical Sciences, Geosciences, and Biosciences Division, Office of the Basic Energy Sciences, Office of Sciences, United States Department of Energy (under grant DE-FG02-97ER14799) for financial support. Florian Garczarek and Klaus Gerwert gratefully acknowledge the support of the Deutsche Forschungsgemeinschaft (GE 599/12-1).

REFERENCES

Anfinrud, P. A., C. Han, and R. M. Hochstrasser. 1989. Direct observations of ligand dynamics in hemoglobin by subpicosecond infrared spectroscopy. *Proc. Natl. Acad. Sci. USA.* 86:8387–8391.

Brown, L. S., J. Sasaki, H. Kandori, A. Maeda, R. Needleman, and J. K. Lanyi. 1995. Glutamic acid 204 is the terminal proton release group at the extracellular surface of bacteriorhodopsin. *J. Biol. Chem.* 270:27122–27126.

Haupts, U., J. Tittor, and D. Oesterhelt. 1999. Closing in on bacteriorhodopsin: progress in understanding the molecule. *Annu. Rev. Biophys. Biomol. Struct.* 28:367–399.

Hayashi, S., and I. Ohmine. 2000. Proton transfer in bacteriorhodopsin: structure, excitation, IR spectra, and potential energy surface analyses by an ab initio QM/MM method. *J. Phys. Chem. B.* 104:10678–10691.

Heberle, J., and N. A. Dencher. 1992. Surface-bound optical probes monitor proton translocation and surface potential changes during the bacteriorhodopsin photocycle. *Proc. Natl. Acad. Sci. USA.* 89:5996–6000.

Kandori, H., N. Kinoshita, Y. Shichida, and A. Maeda. 1998. Protein structural changes in bacteriorhodopsin upon photoisomerization as revealed by polarized ftir spectroscopy. *J. Phys. Chem. B.* 102:7899–7905.

Kandt, C., J. Schlitter, and K. Gerwert. 2004. Dynamics of water molecules in the bacteriorhodopsin trimer in explicit lipid/water environment. *Biophys. J.* 86:705–717.

Kim, J., U. W. Schmitt, J. A. Gruetzmacher, G. A. Voth, and N. E. Scherer. 2002. The vibrational spectrum of the hydrated proton: comparison of experiment, simulation, and normal mode analysis. *J. Chem. Phys.* 116:737–746.

Lanyi, J. K. 2000. Molecular mechanism of ion transport in bacteriorhodopsin: insights from crystallographic, spectroscopic, kinetic, and mutational studies. *J. Phys. Chem. B.* 104:11441–11448.

Le Coutre, J., J. Tittor, D. Oesterhelt, and K. Gerwert. 1995. Experimental evidence for hydrogen-bonded network proton transfer in bacteriorhodopsin shown by Fourier-transform infrared spectroscopy using azide as catalyst. *Proc. Natl. Acad. Sci. USA.* 92:4962–4966.

Lobaugh, J., and G. A. Voth. 1996. The quantum dynamics of an excess proton in water. *J. Chem. Phys.* 104:2056–2069.

Logunov, S. L., M. A. Elsayed, and J. K. Lanyi. 1996. Catalysis of the retinal subpicosecond photoisomerization process ire acid purple bacteriorhodopsin and some bacteriorhodopsin mutants by chloride ions. *Biophys. J.* 71:1545–1553.

Luecke, H., B. Schobert, H. T. Richter, J. P. Cartailler, and J. K. Lanyi. 1999. Structure of bacteriorhodopsin at 1.55 angstrom resolution. *J. Mol. Biol.* 291:899–911.

Olejnik, J., B. Brzezinski, and G. Zundel. 1992. A proton pathway with large proton polarizability and the proton pumping mechanism in bacteriorhodopsin-Fourier transform difference spectra of photoproducts of bacteriorhodopsin and of its pentademethyl analogue. *J. Mol. Struct.* 271:157–173.

Rammelsberg, R., G. Huhn, M. Lubben, and K. Gerwert. 1998. Bacteriorhodopsins intramolecular proton-release pathway consists of a hydrogen-bonded network. *Biochemistry.* 37:5001–5009.

Riesle, J., D. Oesterhelt, N. A. Dencher, and J. Heberle. 1996. D38 is an essential part of the proton translocation pathway in bacteriorhodopsin. *Biochemistry.* 35:6635–6643.

Rousseau, R., V. Kleinschmidt, U. W. Schmitt, and D. Marx. 2004. Modeling protonated water networks in bacteriorhodopsin. *Phys. Chem. Chem. Phys.* 6:1848–1859.

Song, L., M. A. El-Sayed, and J. K. Lanyi. 1993. Protein catalysis of the retinal subpicosecond photoisomerization in the primary process of bacteriorhodopsin photosynthesis. *Science.* 261:891–894.

Spassov, V. Z., H. Luecke, K. Gerwert, and D. Bashford. 2001. pK(a) calculations suggest storage of an excess proton in a hydrogen-bonded water network in bacteriorhodopsin. *J. Mol. Biol.* 312:203–219.

Tanimoto, T., Y. Furutani, and H. Kandori. 2003. Structural changes of water in the Schiff base region of bacteriorhodopsin: proposal of a hydration switch model. *Biochemistry.* 42:2300–2306.

Tittor, J., and D. Oesterhelt. 1990. The quantum yield of bacteriorhodopsin. *FEBS Lett.* 263:269–273.

Vuilleumier, R., and D. Borgis. 1999. Transport and spectroscopy of the hydrated proton: A molecular dynamics study. *J. Chem. Phys.* 111:4251–4266.

Wang, J. P., and M. A. El-Sayed. 2000. Proton polarizability of hydrogen-bonded network and its role in proton transfer in bacteriorhodopsin. *J. Phys. Chem.* 104:4333–4337.

Wang, J., and M. A. El-Sayed. 2001. Time-resolved Fourier transform infrared spectroscopy of the polarizable proton continua and the proton pump mechanism of bacteriorhodopsin. *Biophys. J.* 80:961–971.

Wang, J., and M. A. El-Sayed. 2002. Time-resolved long-lived infrared emission from bacteriorhodopsin during its photocycle. *Biophys. J.* 83:1589–1594.

Zundel, G. 2000. Hydrogen bonds with large proton polarizability and proton transfer processes in electrochemistry and biology. *Adv. Chem. Phys.* 111:1–218.